THE INFLUENCE OF MORPHOLOGY AND TOPOLOGY OF REINFORCEMENTS ON THERMO-ELASTIC PROPERTIES OF COMPOSITES: APPLICATION TO ELECTRONIC COMPONENTS

S. Ben Khlifa[1], W. Kpobie[1,2], N. Bonfoh[1], M. Fendler[2], C. Dreistadt[1], P. Lipinski[1*]

[1]*Laboratoire de Mécanique Biomécanique Polymère Structures (LaBPS) - EA 4632, Ecole Nationale d'Ingénieurs de Metz (ENIM) –1 route d'Ars Laquenexy CS 65820, 57078 Metz Cedex 3, France*
[2]*Laboratoire d'Electronique et des Technologies de l'Information, CEA / LETI-MINATEC, 17, rue des Martyrs, 38004 Grenoble.*
** E-mail address: lipinski@enim.fr (P. Lipinski)*

Keywords: micromechanics, multi-site approach, thermo-elastic, finite elements.

Abstract
A micromechanical multi-site modelling of the effective thermo-elastic properties of heterogeneous materials, derived from the classical integral equation is proposed. The fundamental solution based on the Green function of elasticity problem is used to derive a general expression of elastic and thermal strain concentration tensors. This last one enables the development of specific models such as multi-site Mori-Tanaka, Self-consistent or Generalized Self-Consistent schemes. The main advantage of the model resides in its capability to take into account the morphological as well as the topological material micro-architecture. The proposed model is implemented in finite elements software in order to analyse the reliability of electronic assemblies such as flip-chips.

1 Introduction
In many industrial applications composite materials are frequently subjected to thermo-mechanical loads. For the special case of a flip-chip assembly made of different materials, its reliability requires a precise estimation of its overall thermo-mechanical behaviour. From the considered microstructure, homogenisation approaches based on the Eshelby equivalent-inclusion concept [1], can be used for this purpose. The determination of thermo-elastic behaviour of micro-heterogeneous materials has been partially investigated since initial works of Levin [2], Hill [3] and Kröner [4].
The original Mori-Tanaka approach [5] was suggested for composites with reinforcements of similar shape. For two or multi-phase composites containing inclusions with similar shape and alignment, Benveniste et al. [6], established that the Mori-Tanaka and the self-consistent approaches lead to a diagonally symmetric effective stiffness tensor.
The present work aims to propose an alternative micromechanical formulation based on a multi-site formulation of the Mori-Tanaka approach. Applied to biphasic composites, the provided modelling allowed analysing the effects of morphology and topology of reinforcements on the equivalent behaviour. Finally, the corresponding model is implemented for finite elements calculations related to a flip chip assembly in order to analyse its reliability.

2 Multi-site micromechanical modelling
The global properties of a micro-heterogeneous material can be determined knowing the strain localisation tensors. Let's consider a heterogeneous material with its local constitutive

relation specifying the stress $\boldsymbol{\sigma}(\boldsymbol{r})$ in function of the total strain $\boldsymbol{\varepsilon}(\boldsymbol{r})$ and homogeneous temperature increment θ:

$$\boldsymbol{\sigma}(\boldsymbol{r}) = \boldsymbol{c}(\boldsymbol{r}) : \boldsymbol{\varepsilon}(\boldsymbol{r}) - \theta\boldsymbol{\beta}(\boldsymbol{r}) \tag{1}$$

where $\boldsymbol{c}(\boldsymbol{r})$ and $\boldsymbol{\beta}(\boldsymbol{r})$ are respectively local elastic and thermal properties of the considered material. Following the approach developed by Ahaouari [7] and Ahaouari et al. [8], a thermo-mechanical integral equation can be established:

$$\boldsymbol{\varepsilon}(\boldsymbol{r}) = \boldsymbol{E}^r - \int_V \boldsymbol{\Gamma}(\boldsymbol{r}-\boldsymbol{r}') : \left[\delta\boldsymbol{c}(\boldsymbol{r}') : \boldsymbol{\varepsilon}(\boldsymbol{r}') - \theta\delta\boldsymbol{\beta}(\boldsymbol{r}')\right] dV' \tag{2}$$

where $\boldsymbol{\Gamma}(\boldsymbol{r}-\boldsymbol{r}')$ is the modified Green tensor, deduced from the Green's displacement tensor $\boldsymbol{G}$ of an infinite homogeneous reference medium ($\boldsymbol{c}^r$, $\boldsymbol{\beta}^r$):

$$\Gamma_{ijkl}(\boldsymbol{r}-\boldsymbol{r}') = -\frac{1}{2}\left[G_{ik,jl}(\boldsymbol{r}-\boldsymbol{r}') + G_{jk,il}(\boldsymbol{r}-\boldsymbol{r}')\right] \tag{3}$$

Deviations of local thermo-elastic properties with respect to this reference medium are defined as:

$$\begin{cases} \delta\boldsymbol{c}(\boldsymbol{r}) = \boldsymbol{c}(\boldsymbol{r}) - \boldsymbol{c}^r \\ \delta\boldsymbol{\beta}(\boldsymbol{r}) = \boldsymbol{\beta}(\boldsymbol{r}) - \boldsymbol{\beta}^r \end{cases} \tag{4}$$

As developed by Kpobie et al. [9], Eq. (2) leads to a system of algebraic equations for the unknown total strain of each constituent $\boldsymbol{\varepsilon}^I$:

$$\boldsymbol{\varepsilon}^I = \boldsymbol{E}^r - \sum_{J=1}^{N} \boldsymbol{T}^{IJ}\left(\boldsymbol{c}^R\right) : \left(\Delta\boldsymbol{c}^J : \boldsymbol{\varepsilon}^J - \theta\Delta\boldsymbol{\beta}^J\right) \qquad I = 1, 2, ..., N \tag{5}$$

The tensor $\boldsymbol{T}^{IJ}\left(\boldsymbol{c}^r\right)$ describing mechanical interactions between constituents through the reference medium $\boldsymbol{c}^r$, is called "interaction tensor":

$$\boldsymbol{T}^{IJ}\left(\boldsymbol{c}^r\right) = \frac{1}{V^I}\int_{V^I}\int_{V^J} \boldsymbol{\Gamma}\left(\boldsymbol{r}-\boldsymbol{r}'\right) dV' dV \tag{6}$$

The solution of Eq. (5) is expressed in terms of localisation operation with respect to the strain of reference medium $\boldsymbol{E}^r$ and the temperature increment θ as:

$$\boldsymbol{\varepsilon}^I = \boldsymbol{R}^I : \boldsymbol{E}^r + \theta\boldsymbol{r}^I \tag{7}$$

The considered case concerns a matrix ($\boldsymbol{c}^M$ and $\boldsymbol{\beta}^M$) containing ellipsoidal inclusions with the same shape, alignments and thermo-elastic properties ($\boldsymbol{c}$ and $\boldsymbol{\beta}$). Inclusions can be arranged in various ordered manner as illustrated by Fig. 1a, where l_1, l_2 (and l_3) are distances in three orthogonal directions between the centres of neighbouring inclusions.

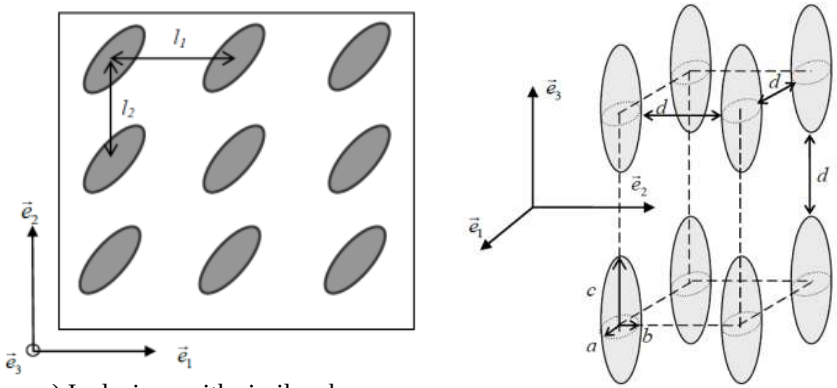

a) Inclusions with similar shape

b) 3D spatial arrangement of reinforcements

Figure 1. Two-phase ordered composite material

To take into account the topological texture of the composite, interactions of these *N-1* inclusions are considered. Moreover, the total volume fraction of inclusions is denoted $f = \sum_{I=2}^{N} f_I$. Localisation tensors are therefore identical for all considered inclusions. In this considered case, following expressions hold true:

$$\begin{aligned} \boldsymbol{R}^I &= \left(\boldsymbol{I} + \boldsymbol{T}^I : \Delta\boldsymbol{c}\right)^{-1} \\ \boldsymbol{r}^I &= \left(\boldsymbol{I} + \boldsymbol{T}^I : \Delta\boldsymbol{c}\right)^{-1} : \boldsymbol{T}^I : \Delta\boldsymbol{\beta} = \boldsymbol{R}^I : \boldsymbol{T}^I : \Delta\boldsymbol{\beta} \end{aligned} \tag{8}$$

Consequently, localisation tensors with respect to the imposed macroscopic thermo-mechanical loading ($\boldsymbol{E}$ and θ) introduced as $\boldsymbol{\varepsilon}^I = \boldsymbol{A}^I : \boldsymbol{E} + \theta\boldsymbol{a}^I$ leads to:

$$\begin{aligned} \boldsymbol{A}^M &= \left[\boldsymbol{I} - f\left(\boldsymbol{I} - \boldsymbol{R}^I\right)\right]^{-1} \\ \boldsymbol{a}^M &= -f\,\boldsymbol{A}^M : \boldsymbol{r}^I \end{aligned} \tag{9}$$

For the matrix and:

$$\begin{aligned} \boldsymbol{A}^I &= \left[\boldsymbol{I} + (1-f)\boldsymbol{T}^I : \Delta\boldsymbol{c}\right]^{-1} \\ \boldsymbol{a}^I &= \boldsymbol{r}^I - \boldsymbol{A}^I : \overline{\boldsymbol{r}^I} = \boldsymbol{r}^I - f\,\boldsymbol{A}^I : \boldsymbol{r}^I = (1-f)\boldsymbol{A}^M : \boldsymbol{r}^I = \frac{1-f}{f}\boldsymbol{a}^M \end{aligned} \tag{10}$$

for all inclusions. Accordingly, global thermo-elastic properties of the composite are deduced from following relations:

$$\begin{aligned} \boldsymbol{C}^{GMT} &= \boldsymbol{c}^M + f\Delta\boldsymbol{c} : \boldsymbol{A}^I = \boldsymbol{c}^M + f\Delta\boldsymbol{c} : \boldsymbol{R}^I : \boldsymbol{A}^M \\ \boldsymbol{\beta}^{GMT} &= \boldsymbol{\beta}^M + f\left(\Delta\boldsymbol{\beta} - \Delta\boldsymbol{c} : \boldsymbol{a}^I\right) = \boldsymbol{\beta}^M + f\left[\Delta\boldsymbol{\beta} + \Delta\boldsymbol{c} : \left(\boldsymbol{A}^M : \boldsymbol{r}^I + \boldsymbol{a}^M\right)\right] \end{aligned} \tag{11}$$

3 Applications

3.1 Influence of topology and morphology of reinforcements

This section aims to analyse predictions of the proposed model. Especially, the estimation of equivalent thermo-elastic properties as a function of reinforcements' topology and morphology is performed.

A cubic topology of reinforcements is analysed. Only the first neighbours, i.e. 26 *J*-inclusions surrounding a selected *I*-inclusion, are taken into account. A typical spatial arrangement of such a composite is illustrated in Fig. 1b. The same figure indicates the main geometric parameters introduced in this study. *a*, *b* and *c* are semi-axes of the ellipsoidal reinforcement and *d* the distance between poles of two adjacent inclusions. This distance is supposed to be the same in $\vec{e}_1$, $\vec{e}_2$ and $\vec{e}_3$ directions. Moreover, to simplify analysis, only the case of inclusions with circular cross section is considered ($a = b$) and two dimensionless parameters, namely $\kappa = c/a$ and $\delta = d/a$ are introduced. Computed simulations concern a composite material made of an Aluminium matrix reinforced by silicon carbide inclusions. Thermo-elastic properties are assumed isotropic for both phases are gathered in Table 1.

Property	Inclusion (SiC)	Matrix (Al)
Young's modulus (GPa)	700	70
Poisson's ratio	0.27	0.3
CTE (10^{-6} K^{-1})	4	21

Table 1. Mechanical properties of the local phases

Considered reinforcements are supposed spherical ($\kappa=1$) and consequently the tensor of global elastic properties is expected to possess cubic material symmetries. In such a situation, the elastic anisotropy of the material can be estimated by the following parameter:

$A_C = \dfrac{C_{1111}^{GMT}}{C_{1122}^{GMT} + 2C_{1212}^{GMT}}$ the value of which is guessed to be influenced by δ related to the volume fraction f of reinforcement.

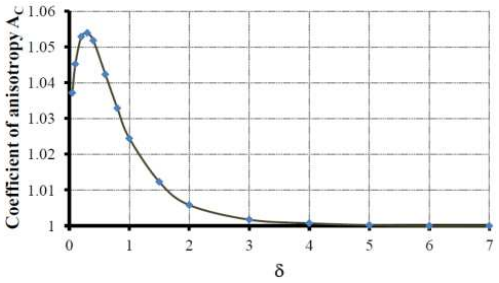

a) Variations of A_C as a function of the parameter δ

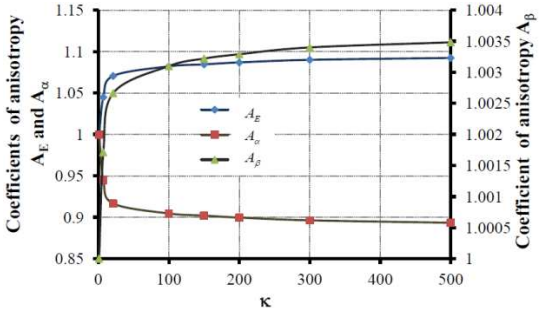

b) Evolution of A_E, A_α and A_β in function of κ for f=0.0122

Figure 2. Variation of coefficients of anisotropy

Fig. 2a shows the evolution of this anisotropy parameter A_C as a function of δ. For relatively close reinforcements $\delta \le 2$, or important volume fraction $f \ge 0.065$, the effective elastic behaviour appears anisotropic ($A_C > 1$). The anisotropy coefficient A_C tends to 1 with an increasing δ. Obviously, this limit value of A_C corresponds to isotropic materials. For $\delta > 4$, the relative distance between spherical inclusions becomes large enough to neglect mutual interactions of neighbouring reinforcements. For such configurations, predicted tensor of elastic moduli exhibits quasi-isotropic properties and tends to the solution of the classical one-site Mori-Tanaka model.

Predictions of the advocated model have also been analysed in light of the morphology of reinforcements. For this purpose, elongated ellipsoidal inclusions with circular cross-sections are considered. To characterise the inclusion morphology, the ratio $\kappa = c/a$ has been varied. Large range of κ has been covered. Since the expected global behaviour of such a composite has no cubic symmetry, the anisotropy of its thermo-elastic properties is evaluated in terms of following factors:

$$A_E = \frac{E_3}{E_1} = \frac{S_{1111}^{GMT}}{S_{3333}^{GMT}}; \quad A_\alpha = \frac{\alpha_{33}^{GMT}}{\alpha_{11}^{GMT}} \quad A_\beta = \frac{\beta_{33}^{GMT}}{\beta_{11}^{GMT}}$$

Reported simulations concern a fixed volume fraction $f \approx 0.0122$. This relatively weak volume fraction has been chosen to limit the influence of the topological microstructure. As it has been concluded in the previous paragraph, for such relative distances between reinforcements, interactions of the adjacent inclusions are practically negligible. Fig. 2b depicts the evolution of the anisotropy coefficients as functions of the morphology κ.

Effective thermo-elastic properties are evidently affected by the shape of considered inclusions. The initial values of the anisotropy coefficients, for $\kappa = 1$, are close to 1 revealing the quasi-isotropic behaviour in the case of spherical reinforcements. They sharply evolve for $1 \le \kappa \le 20$. This evolution becomes practically insignificant for $\kappa > 300$. Such tendency is in agreement with the behaviour suggested by Hutchinson [10].

3.2 Implementation of the thermo-elastic behaviour in a finite elements code

In this section, the implementation of a thermo-elastic constitutive law in a finite element code is presented. The proposed model is implemented in the finite element code ABAQUS ® standard via the user subroutine UMAT. First, the thermo-elastic properties of equivalent material must be determined for each integration point, according to its temperature. Our goal is, for a given time increment, to determine the evolution of all mechanical fields discussed in the preceding section. The procedure used by ABAQUS ®, as the majority of finite element codes, is a numerical treatment by iterations of a discredited version of the principle of virtual power (PVP).

Let's assume that for a current time $t_n \in [0,T]$, following data are converged:

- $\boldsymbol{E}_n$, $\boldsymbol{E}^e_n$, $\boldsymbol{E}^\theta_n$: converged values of the total, elastic and thermal strains respectively,
- $\Delta\boldsymbol{E}$: an increment of total strain.

At the beginning of each increment, the temperature of the material is updated to the value corresponding to the end of the step $n+1$:

$$\theta_{n+1} = \theta_n + \Delta\theta \tag{12}$$

Being a loosely coupled thermo-mechanical problem, this temperature does not change during the Newton-Raphson process for converged solution. Whereupon, following mechanical parameters are computed via the developed model: $\boldsymbol{C}^{GMT}_{n+1}$, $\boldsymbol{\alpha}^{GMT}_{n+1}$ or $\boldsymbol{\beta}^{GMT}_{n+1}$, $\boldsymbol{A}^I_{n+1}$, , $\boldsymbol{A}^M_{n+1}$, $\boldsymbol{a}^I_{n+1}$ and $\boldsymbol{a}^M_{n+1}$. After that, some variables have to be updated as follows:

$$\begin{aligned}
&\boldsymbol{E}_{n+1} = \boldsymbol{E}_{\boldsymbol{n}} + \Delta\boldsymbol{E}, \quad \Delta\boldsymbol{E}^\theta_{n+1} = \Delta\theta\boldsymbol{\alpha}^{GMT}_{n+1} + \theta_n\Delta\boldsymbol{\alpha}^{GMT}_{n+1}, \quad \Delta\boldsymbol{E}^e_{n+1} = \Delta\boldsymbol{E} - \Delta\boldsymbol{E}^\theta_{n+1} \\
&\boldsymbol{E}^e_{n+1} = \boldsymbol{E}^e_{\boldsymbol{n}} + \Delta\boldsymbol{E}^e_{n+1}, \quad \boldsymbol{E}^\theta_{n+1} = \boldsymbol{E}^\theta_{\boldsymbol{n}} + \Delta\boldsymbol{E}^\theta_{n+1} \\
&\Delta\boldsymbol{\Sigma}_{n+1} = \boldsymbol{C}^{GMT}_{n+1} : \Delta\boldsymbol{E}^e_{n+1} + \Delta\boldsymbol{C}^{GMT}_{n+1} : \boldsymbol{\Sigma}_n, \quad \boldsymbol{\Sigma}_{n+1} = \boldsymbol{\Sigma}_n + \Delta\boldsymbol{\Sigma}_{n+1}
\end{aligned} \tag{13}$$

From the localisation tensor introduced by Eq. (10), local strain and stress fields can then be computed for reinforcements for example:

$$\begin{aligned}
&\Delta\boldsymbol{\varepsilon}^I_{n+1} = \boldsymbol{A}^I_{n+1} : \Delta\boldsymbol{E}_{n+1} + \Delta\boldsymbol{A}^I_{n+1} : \boldsymbol{E}_n + \boldsymbol{a}^I_{n+1}\Delta\theta + \Delta\boldsymbol{a}^I_{n+1}\theta_n \\
&\boldsymbol{\varepsilon}^I_{n+1} = \boldsymbol{\varepsilon}^I_n + \Delta\boldsymbol{\varepsilon}^I_{n+1}
\end{aligned} \tag{14}$$

and:

$$\begin{aligned}
&\Delta\boldsymbol{\sigma}^I_{n+1} = \boldsymbol{c}^I_{n+1} : \Delta\boldsymbol{\varepsilon}^I_{n+1} - \Delta\theta\,\boldsymbol{\beta}^I_{n+1} + \Delta\boldsymbol{c}^I_{n+1} : \boldsymbol{\varepsilon}^I_n - \theta_n\,\Delta\boldsymbol{\beta}^I_{n+1} \\
&\boldsymbol{\sigma}^I_{n+1} = \boldsymbol{\sigma}^I_n + \Delta\boldsymbol{\sigma}^I_{n+1}
\end{aligned} \tag{15}$$

In this thermo-elastic problem, the consistent algorithmic module is the Mori-Tanaka tensor $\boldsymbol{C}^{GMT}$ of effective elastic moduli of the homogeneous equivalent material (HEM).

3.3 Finite Elements validation

The flip chip assembly (Fig. 3a) has significant advantages over other microelectronic packaging technologies. It is a high-density and high reliability interconnection technology designed for System-In-Package (SIP) and 3D-WLP (Wafer Level Packaging) applications.

The considered flip-chip assembly consists of three layers: a substrate in fused quartz, a die in silicon and an interconnection layer formed by indium solder bumps coated with epoxy glue. The most important difficulty to model such a structure is the tremendous number of indium bumps due to the periodic structure of the flip-chip. The undesired deflection appearing on the quartz substrate during hybridisation of the components is our main concern. In order to test the relevance of the proposed thermo-elastic model and its implementation, a configuration with only a few balls is considered. Two FE models are built, namely the exact geometric

modelling taking into account the existing balls and the simplified model for which the layer consisting of the indium bumps and the underfill (epoxy) is replaced by an equivalent homogeneous material whose equivalent thermo-elastic properties are determined through the proposed modelling (see fig. 3b)

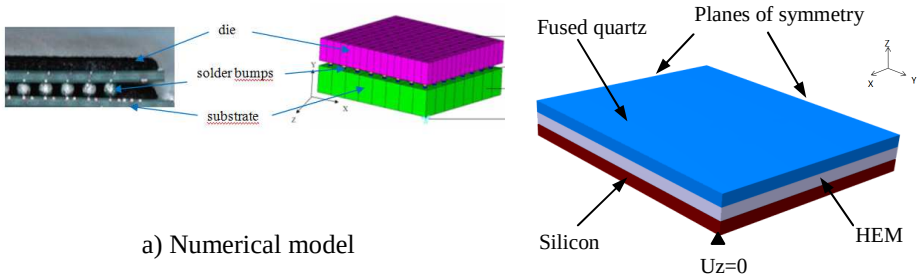

a) Numerical model

b) Boundary conditions

Figure 3. Flip chip assembly

For the range of tested temperature (293K to 400K) and due to amplitude of the remote loading, it is assumed that fused silica and silicon behave in purely elastic manner. The behaviours of indium and epoxy are also assumed elastic in this analysis. Corresponding properties of constituents of the flip-chip are listed in Tab.3 for three temperatures T= 293, 350 and 400K.

	Coefficient of thermal expansion (10^{-6} K^{-1})			**Young's modulus (GPa)**			**Poisson's ratio**		
Temperature	293 K	350 K	400 K	293 K	350 K	400 K	293 K	350 K	400 K
Fused quartz	0.461	0.57	0.61	72.595	73.376	73.983	0.17	0.172	0.174
Silicon	2.527	2.97	3.25	130.43	129.88	129.4	0.276	0.276	0.276
Indium	29.2	32	33	13.684	11.496	9.584	0.469	0.474	0.45
Epoxy	73	100	139	3.664	4.2	4.5	0.258	0.32	0.3

Table 3. Thermo-elastic parameters of flip chip assembly materials

The footprint of these chips is: 150 x 150 µm^2. The silicon and fused silica layers are 10µm thick and the interconnection layer (indium solder bumps + epoxy) thickness is 8 µm.
All specimens were meshed using ABAQUS finite element code. Due to symmetries of the problem, only ¼ of the package is modelled using 8-node hexahedral elements of ABAQUS library.
The thermo-mechanical boundary conditions applied to the model are illustrated in Fig. 3b.
•Mechanical boundary conditions: Faces 1 and 2: $U_x = 0$ and $U_y = 0$ (Planes of symmetry) and corner node: $U_z = 0$
•Thermal boundary conditions: cooling from 430K to 293K

The finite element mesh is shown in Figure 4a. Two numerical models of the flip-chip assembly have been considered:

- model with indium balls and epoxy (fig. 4) and,
- model with homogeneous equivalent material representing indium balls and epoxy layer (fig. 5).

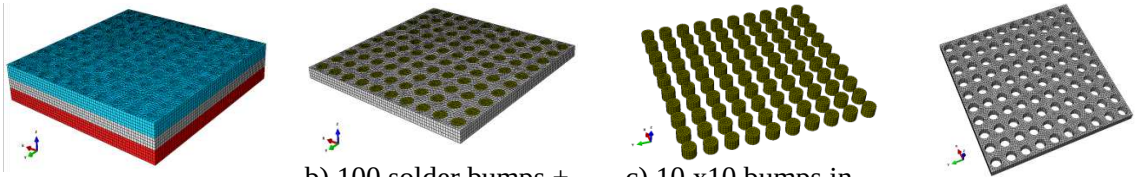

a) Model with solder bumps

b) 100 solder bumps + epoxy

c) 10 x10 bumps in pitch of 15µm x 15µm

d) Epoxy

Figure 4. Geometrically exact model (intermediate layer composed of indium balls + epoxy, 117628 elements)

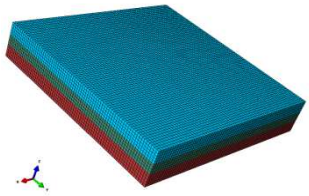

Figure 5. Model with homogeneous equivalent material (78750 elements)

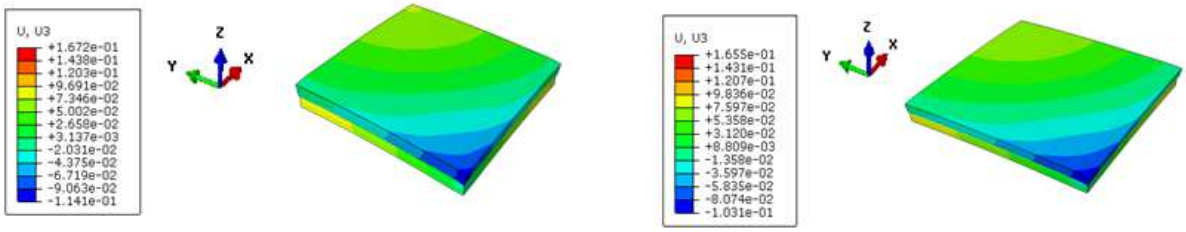

a) Model with solders bumps

b) Model with HEM

Figure 6. Vertical displacement of two samples

Fig. 6 summarises the obtained results in terms of the vertical displacement of the assembly. The maximum vertical displacement on quartz for the exact model with indium balls and epoxy is about 0.1779µm while that provided by the model with equivalent material is 0.1725µm. The relative difference between the two numerical models is 3%. The developed homogenisation model seems relevant to well describe the macroscopic behaviour of the flip-chip assembly.

Analysing the von-Mises stress field in the indium bumps as depicted by fig. 7, similar contours for both approaches can be noticed. The maximum values are localised at interfaces between the bumps and the substrates and are liable to induce failures in these assemblies (disconnection, cracks ...). Currently these types of electronics assembly have a very large number of solder bumps (1024 x 1024 indium balls) which makes it nearly impossible to model. The proposed approach has the main advantage to allow this kind of simulations.

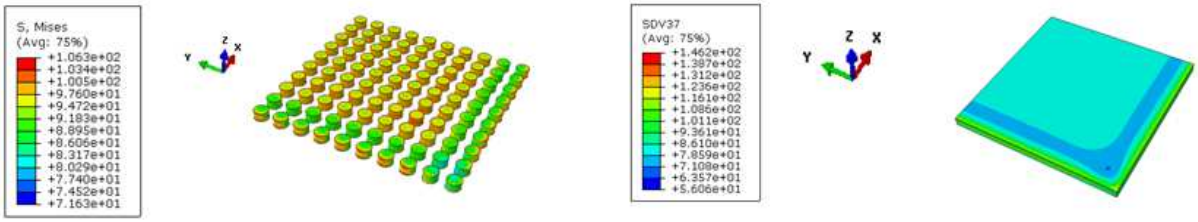

a) Model with solders bumps

b) Model with HEM

Figure 7. Von Mises stress in the solder bumps

Conclusion

Based on the integral equation established in thermo-elasticity, a general model of predictions of the effective properties of composites with ellipsoidal reinforcements and taking into account their morphology and topology is proposed. Thus, a multi-site Mori-Tanaka thermo-elastic scheme has been derived from this solution. A particular model for two-phase composite with periodic arrangement of inclusions has been deduced from the latter one. To uncouple the effect of inclusions' morphology and topology on resulting composite anisotropy, calculations have been performed for two distinct configurations. First one concerned composites with isotropic (spherical) inclusions, the second one with ellipsoidal elongated and sufficiently separated inclusions. We then apply our model to an electronic assembly (flip-chip) consisting of an interconnection layer treated as a two-phase composite. The implementation of the predicted constitutive law of the equivalent homogeneous material of the interconnection layer was made in the Abaqus finite element software. The simulations were performed on two models: one containing 100 indium bumps embedded in epoxy matrix and the other with the equivalent homogeneous material. A relative difference of 3% was found for predicted values of vertical displacement. This precision proves the relevance of the developed homogenisation model and its implementation into finite elements software.

References

[1] Eshelby JD. The determination of the elastic field of an ellipsoidal inclusion, and related problems. *Proc Roy Lond Ser A, Math Phys Sci*; **241**(1226):376-96 (1957).

[2] Levin VM. Thermal expansion coefficients of heterogeneous materials. *Mekhanica Tverdogo Tela* ; **2**:88–94 (English translation: *Mech. Solids* **11**:58–61) (1967).

[3] Hill R. Elastic properties of reinforced solids: some theoretical principles. *J. Mech. Solids*;**11**:357-372 (1963).

[4] Kröner E. Zur Klassichen Theorie Statistisch aufgebauter Festkörper. *Int. J. Engng Sci.*;**11**:171-191(1973).

[5] Mori T, Tanaka K. Average stress in matrix and average elastic energy of materials with misfitting inclusions. *Acta Metallurgica;* **21**:571-574 (1973).

[6] Benveniste Y, Dvorak GJ, Chen T. On diagonal and elastic symmetry of the approximate effective stiffness tensor of heterogeneous media. *J. Mech. Phys. Solids* ; **39** : 927-946 (1991).

[7] Ahaouari K. Contribution à la modélisation de la thermoélasticité et de l'acoustoélasticité des matériaux microhétérogènes, Thèse de l'Université de Metz (1990).

[8] Ahaouari K, Corvasce F, Lipinski P, Berveiller M. Détermination des propriétés thermomécaniques des composites à matrice métallique, *Mémoires et Etudes Scientifiques, Revue de Métallurgie* ; **87** :73-84 (1990).

[9] W. Kpobie, S. Ben Khlifa, N. Bonfoh, M. Fendler, P. Lipinski, Multi-site micromechanical modelling of thermo-elastic properties of heterogeneous materials, *Composite Structures*, **Volume 94**, Issue 6, Pages 2068-2077, (May 2012).

[10] Hutchinson JW. Elastic-plastic behavior of polycrystalline metals and composites. *Proc. Roy. Soc. London, Ser. A*; **319**:247-272 (1970).